doi:10.1016/j.jmb.2006.05.074 J. Mol. Biol. (2006) 361, 33–45

JMB

Available online at www.sciencedirect.com

SCIENCE DIRECT®

ELSEVIER

Non-nucleoside Inhibitors Binding to Hepatitis C Virus NS5B Polymerase Reveal a Novel Mechanism of Inhibition

Bichitra K. Biswal[1], Meitian Wang[1], Maia M. Cherney[1], Laval Chan[2] Constantin G. Yannopoulos[2], Darius Bilimoria[2] Jean Bedard[2] and Michael N. G. James[1]*

[1]*Canadian Institutes of Health Research (CIHR) Group in Protein Structure and Function Department of Biochemistry University of Alberta Edmonton, Alberta Canada T6G 2H7*

[2]*ViroChem Pharma Inc. 275 Armand Frappier Boulevard, Laval, Quebec Canada H7V 4A7*

**Corresponding author*

The RNA-dependent RNA polymerase (NS5B) from hepatitis C virus (HCV) is a key enzyme in HCV replication. NS5B is a major target for the development of antiviral compounds directed against HCV. Here we present the structures of three thiophene-based non-nucleoside inhibitors (NNIs) bound non-covalently to NS5B. Each of the inhibitors binds to NS5B non-competitively to a common binding site in the "thumb" domain that is ~35 Å from the polymerase active site located in the "palm" domain. The three compounds exhibit IC_{50} values in the range of 270 nM to 307 nM and have common binding features that result in relatively large conformational changes of residues that interact directly with the inhibitors as well as for other residues adjacent to the binding site. Detailed comparisons of the unbound NS5B structure with those having the bound inhibitors present show that residues Pro495 to Arg505 (the N terminus of the "T" helix) exhibit some of the largest changes. It has been reported that Pro495, Pro496, Val499 and Arg503 are part of the guanosine triphosphate (GTP) specific allosteric binding site located in close proximity to our binding site. It has also been reported that the introduction of mutations to key residues in this region (i.e. Val499Gly) ablate *in vivo* sub-genomic HCV RNA replication. The details of NS5B polymerase/inhibitor binding interactions coupled with the observed induced conformational changes provide new insights into the design of novel NNIs of HCV.

© 2006 Elsevier Ltd. All rights reserved.

Keywords: hepatitis C virus; RNA-dependent RNA polymerase; non-nucleoside inhibitor; allosteric inhibitor binding site; enzyme inhibition

Introduction

Hepatitis C virus (HCV) chronically infects about 170 million people, ≈3% of the world's population.[1] There is compelling evidence that within 10 to 20 years, this chronic infection progresses to cirrhosis then to hepatocellular carcinoma in about 20% and 5%, respectively, of these infected individuals. Chronic infection by HCV is the leading cause of liver transplantation in USA. To date, there is no vaccine available against HCV. Furthermore, the currently available treatment (a combination of interferon-α and ribavirin) is expensive and effective in only 50–60% of patients treated.[2] The development of new effective antiviral compounds for combating this debilitating human pathogen is therefore of paramount importance and is currently an intensive area of pharmaceutical research.

HCV is a positive-sense single-stranded RNA virus that belongs to the Flaviviridae family. The virus exists in six major genotypes; genotype 1 is the most prevalent one in North America, Europe and Japan. The HCV genome encodes a large polyprotein comprised of about 3000 amino acid residues. Subsequently, the polyprotein is processed by

Present address: M. Wang, Paul Scherrer Institut/SLS, 5232 Villigen PSI, Switzerland.

Abbreviations used: HCV, hepatitis C virus; NNI, non-nucleoside inhibitor; GTP, guanosine triphosphate.

E-mail address of the corresponding author: Michael.james@ualberta.ca

0022-2836/$ - see front matter © 2006 Elsevier Ltd. All rights reserved.

cellular and viral proteases into at least ten individual functional proteins (C, E1, E2, P7, NS2, NS3, NS4A, NS4B, NS5A and NS5B).[3–5] Among these products, NS3, the serine proteinase and NS5B, the RNA-dependant RNA polymerase are the most essential enzymes involved in replication of the viral RNA. Hence these two enzymes are considered as important drug targets by several ongoing drug discovery programs.

Crystal structures of the HCV apopolymerase and of its complexes with nucleotide substrates have been determined and analyzed.[6–10] The three-dimensional structure of HCV polymerase determined from several different crystal forms, resembles a right hand with a characteristic fingers, palm and thumb domain organization, similar to the architectures of the RNA polymerases of polio virus, bacteriophage Φ6, rabbit hemorrhagic disease virus, bovine viral diarrhea virus, and human rhino virus.[11–17] Recently, many non-nucleoside inhibitors (NNIs) of HCV NS5B RNA polymerase have been discovered.[18–29] Structural studies of HCV NS5B polymerase genotypes 1b and 2a in complex with phenylalanine, dihydropyranone, thiophene, and

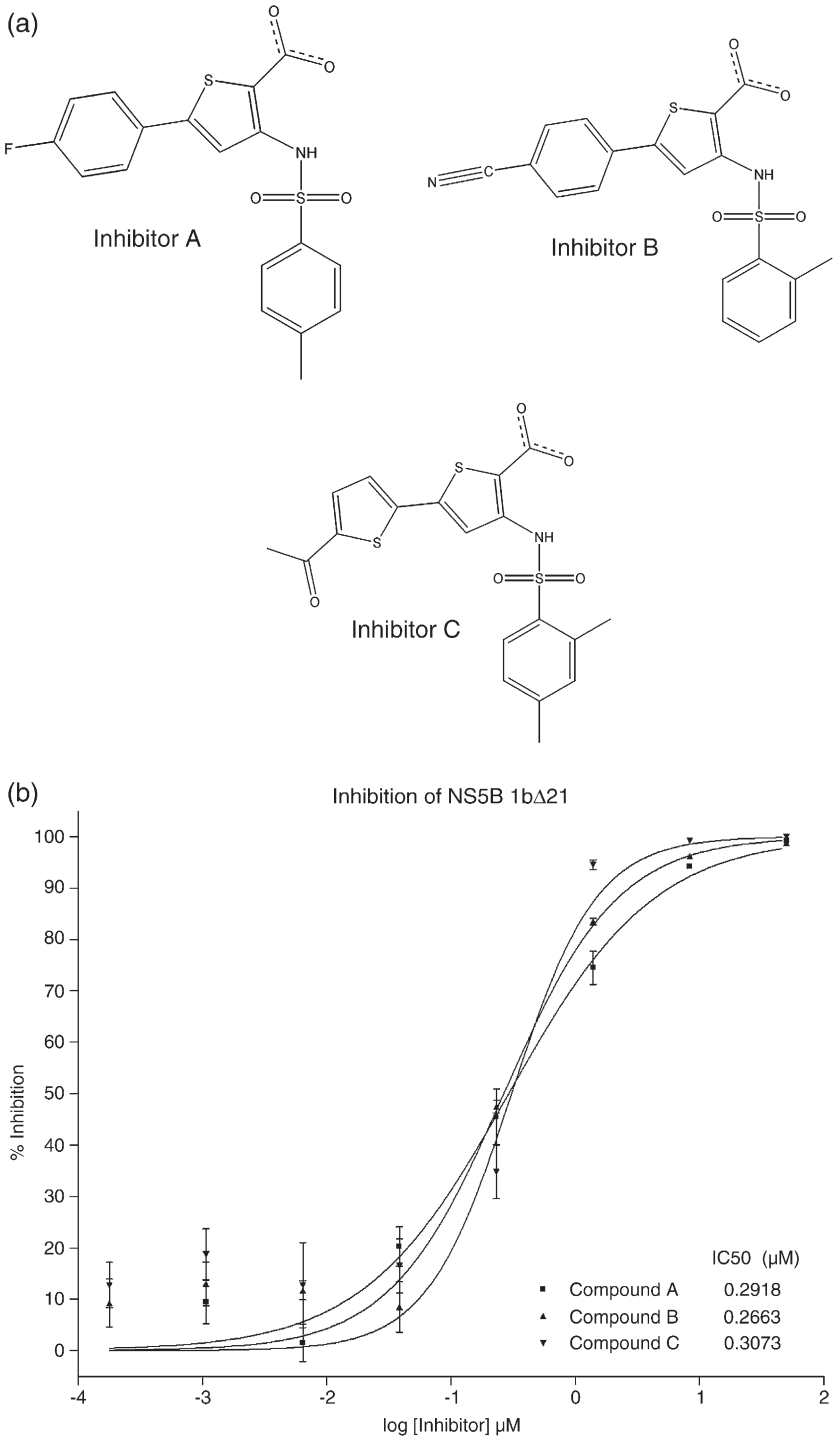

Figure 1. (a) Chemical structures of the non-nucleoside inhibitors A, B and C. (b) Inhibition plot of the inhibition of polymerase in the presence of A, B, or C. NS5B activity was measured as described in Materials and Methods using poly(rA)/oligo(d)T_{15} as template/primer. Reactions were performed in the presence of 30 μM UTP substrate and in the absence or presence of increasing concentrations (0.024 μM to 50 μM) of inhibitors. The inhibition experiments were performed in quadruplicate runs.

indole-based non-nucleoside analogue inhibitors bound non-covalently have also been carried out.[30–34] These studies revealed that phenylalanine, dihydropyranone and thiophene-based non-nucleoside inhibitors bind to a common predominantly hydrophobic depression in the thumb domain, that is located approximately 35 Å from the polymerase active site.[30–32] Close examination of the phenylalanine, dihydropyranone and indole genotype 1b complexes and the thiophene-genotype 2a complex revealed no large local conformational changes in their respective binding pockets. As well no movements were observed for the indole-based NNI pocket on genotype 1b, but the binding of these inhibitors prevented the interaction of the finger-tip (a small α-helix A) of the Λ1 loop to the thumb domain.[33] Based on our genotype 2a work,[32] Di Marco *et al.* proposed that although the indole inhibitors do not cause local perturbations, they act by disrupting the Λ1 loop interaction with the thumb domain thereby freezing the enzyme in some undefined inactive form.[33]

Although previous X-ray analyses of NS5B in complex with other non-covalently bound non-nucleoside inhibitors have provided a wealth of information on the existence of allosteric inhibitor binding sites, no single precise mechanism of inhibition could be deduced. Here, we report the crystal structures of the NS5B polymerase from the HCV genotype 1b in complex with three new thiophene-based sulfonamide NNIs (Figure 1(a)) that were synthesized based on structure activity relationship studies. The details of the inhibitor binding site, inhibitor/enzyme interactions, conformational changes and possible mechanisms of inhibition form the theme of this paper.

Results and Discussion

Effects of non-nucleoside inhibitors on NS5B activity

Compounds A, B, and C (Figure 1(a)) were tested for anti-HCV polymerase genotype 1b activity using NS5B Δ21, a C-terminally truncated form of the enzyme with poly(rA)/oligo(dT)$_{15}$ as a homopolymeric template/primer. In this assay, all compounds were found to inhibit NS5B polymerase activity in a dose-dependent manner with IC_{50} values of 0.29, 0.27, and 0.31 μM for compounds A, B, and C, respectively (Figure 1(b)). Dixon plot analysis has demonstrated the non-competitive nature of the inhibition with respect to UTP as the substrate; the estimated K_i values are 0.23, 0.12, and 0.15 μM for inhibitors A, B, and C, respectively.

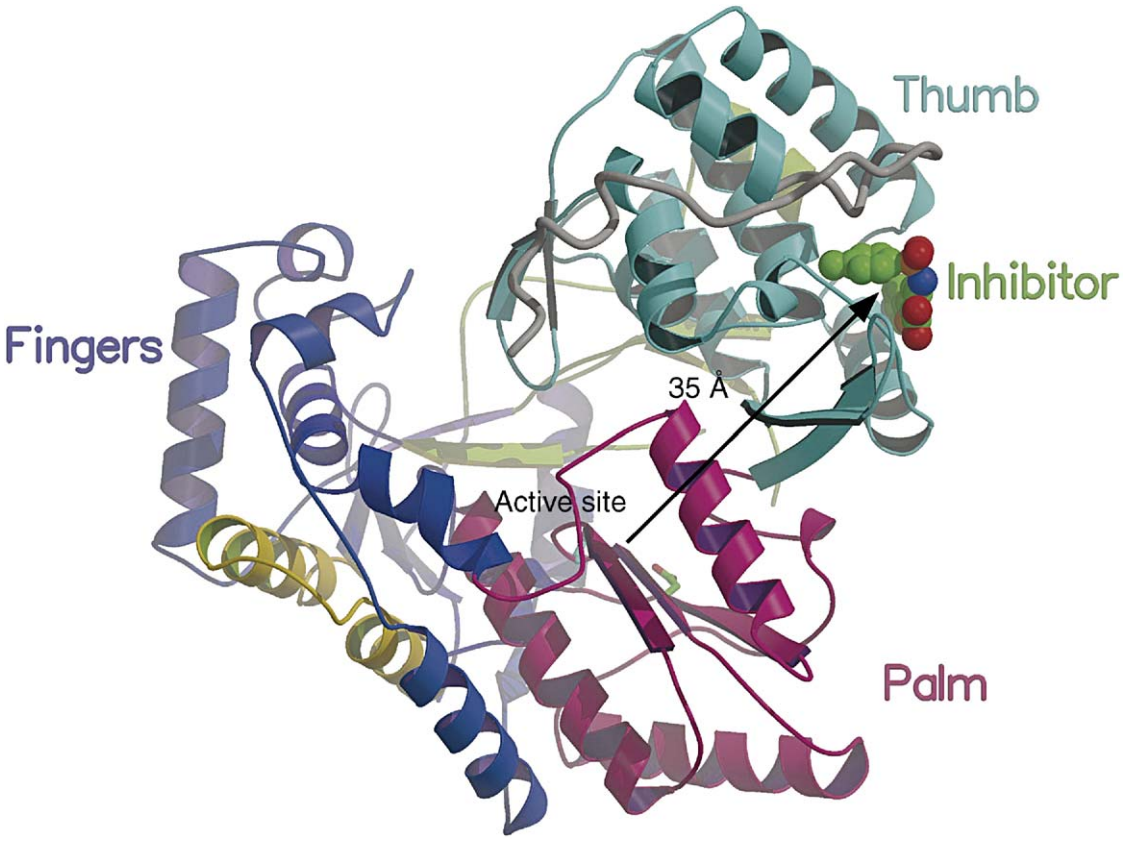

Figure 2. NS5B/inhibitor A complex structure, showing the characteristic fingers, palm, and thumb domains in blue, pink, and cyan, respectively. Two antiparallel α-helices connecting the fingers and palm domains are shown in gold. The inhibitor A bound at the thumb domain is shown in a Corey, Pauling, Koltun (CPK) space-filling model with carbon atoms in green.

Inhibitor binding site and NS5B/inhibitor interaction

Our structural studies of NS5B/inhibitor complexes were carried out on crystals belonging to space group $P2_12_12_1$, the asymmetric unit of which contains two crystallographically independent NS5B polymerase molecules. Each inhibitor binds non-covalently to both molecules in the asymmetric unit, at a predominantly hydrophobic shallow pocket in the thumb domain, that is approximately 35 Å from the polymerase active site located in the palm domain (Figure 2). Binding these inhibitors buries a solvent accessible surface area on the protein of ≈750 Å^2, calculated using a probe radius of 1.4 Å. All functional groups of the inhibitors are well defined in the electron density maps (Figure 3(a), (b) and (c)), indicating well-ordered and tight binding to the polymerase, in agreement with the observed relatively low K_i values. The average *B*-factor of the inhibitor atoms is similar to those of the protein atoms, providing additional evidence for tight binding. The residues lining the binding pocket are Leu419, Arg422, Met423, Leu474, His475, Ser476, Tyr477, Ile482, Ala486, Leu489, Leu497, Arg501, and Trp528; these residues are conserved across all the genotypes of HCV. The fluorophenyl thiophene, cyanophenyl thiophene, and acetyl bithiophene moieties of inhibitors A, B, and C, respectively, are bound to a hydrophobic surface of the thumb domain (Figure 3(a), (b) and (c)). These groups make extensive van der Waals interactions with Leu419, Met423, Ile482, Ala486, Leu489, and Leu497. The oxygen atom of the acetyl group of inhibitor C is hydrogen bonded to the main-chain amide nitrogen atom of Leu497. On the other end of the inhibitors, the 4-methylphenyl, 2-methylphenyl, and 2,4-dimethylphenyl moieties point towards the interior of the thumb domain, filling the primary binding cavity by making extensive van der Waals interactions with Leu419, Met423, Leu474, His475, and Trp528. One of the sulfonyl oxygen atoms of inhibitors A and C is hydrogen bonded to the guanidinium group of Arg501. In general, all the inhibitors bind in a similar fashion (Figure 4) and the nature of the interactions is mainly hydrophobic with the exception of the two common hydrogen bonds received by the carboxylate group of each inhibitor from the main-chain nitrogen atoms of Ser476 and Tyr477 (Figure 5(a) and (b)).

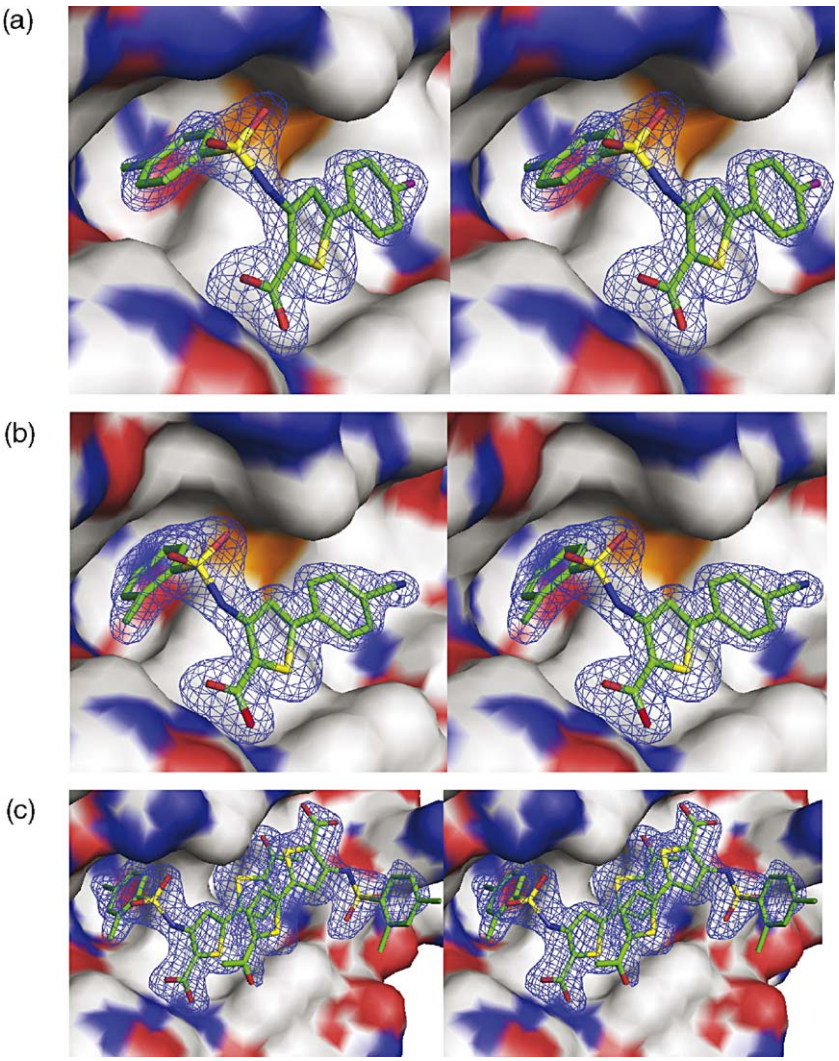

Figure 3. Stereo views of simulated annealed omit $|F_o|-|F_c|$ electron density maps contoured at the 3σ level for the (a) inhibitor A, (b) inhibitor B and (c) inhibitor C. The inhibitors are shown by stick representation with carbon, nitrogen, oxygen, and sulfur atoms in green, blue, red, and yellow, respectively. The inhibitor binding site is shown by a surface representation with carbon, nitrogen, and oxygen atoms in gray, blue, and red, respectively.

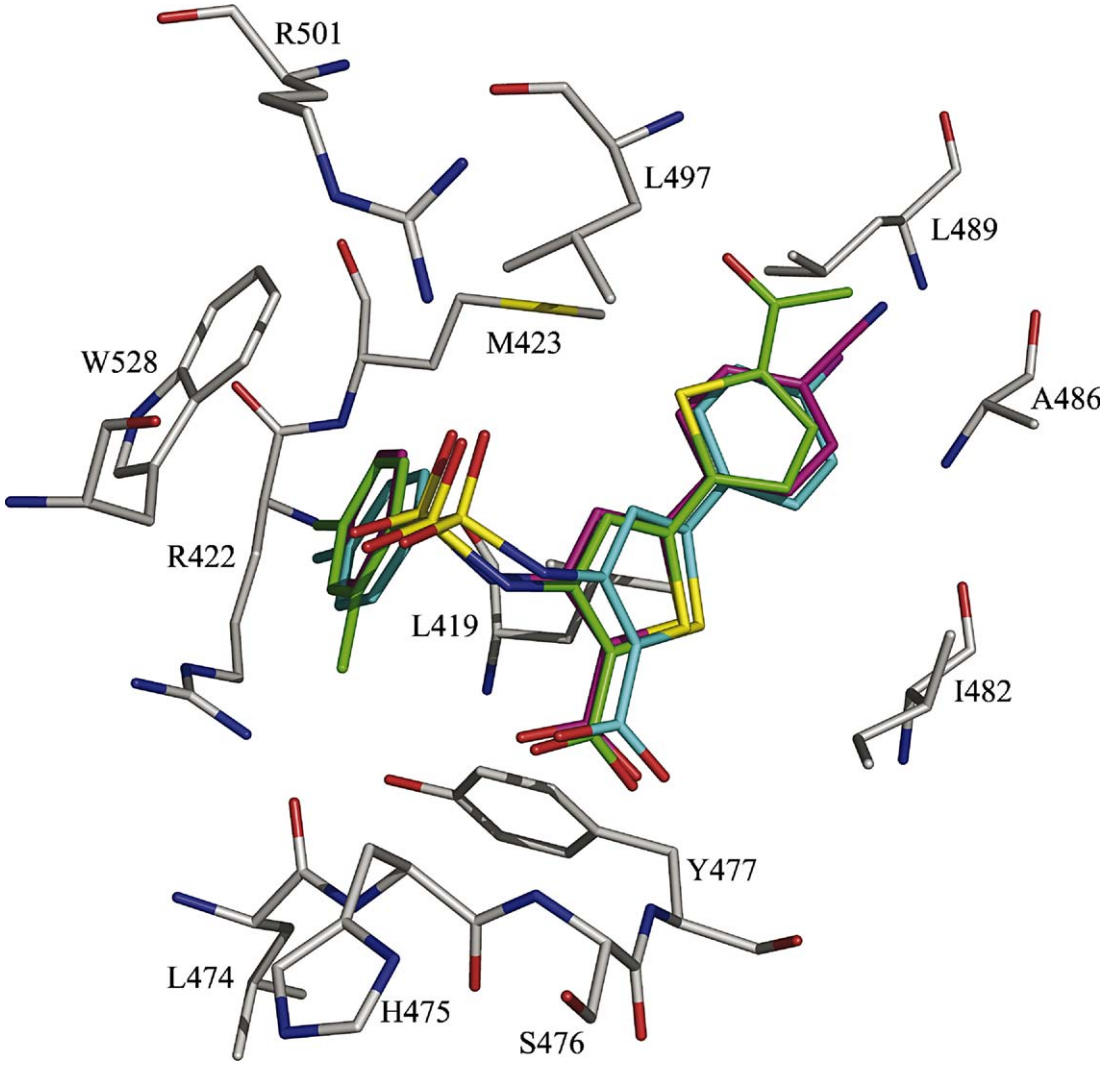

Figure 4. Superimposition of NS5B/inhibitors A, B and C structures, showing the common mode of inhibitor binding. The residues in the inhibitor binding site are shown by stick representation with carbon, nitrogen, oxygen, and sulfur atoms in gray, blue, red, and yellow, respectively. The inhibitors A, B and C are shown by stick representation with their carbon atoms in cyan, magenta and green, respectively.

For inhibitor C, we observed a 2:1 binding stoichiometry (Figures 3(c) and 5(b)) in which one of the inhibitors interacts with the site essentially as described above for A and B, but a second inhibitor molecule stacks against the first one in a reversed orientation forming thiophene/thiophene ring intermolecular interactions. These latter interactions are aromatic in nature with the thiophene planes separated by ~3.4 Å. The second molecule of inhibitor C forms hydrogen bonding and van der Waals interactions with residues Ala486, Arg490, Pro496 and Leu497. The two molecules represent two different conformations of inhibitor C. Both molecules can be superimposed by a 2-fold rotation along an axis perpendicular to the thiophene plane and a rotation of the 2,4-dimethylphenyl moiety by ~160° along N–S bond followed by a translation. The neighboring molecules in the crystal lattice have very little effect on the binding of inhibitor C.

Conformational changes of NS5B upon inhibitor binding and mechanisms of inhibition

To make the structural comparison more meaningful, we have also determined the three-dimensional structure of apo-NS5B polymerase at 1.9 Å from one of the native crystals used in the soaking experiments. The final refined native structure agrees very well with the reported apo-NS5B structure[8] (Root mean square deviation between the two, 0.18 Å, for the 530 C^{α} atom pairs). In order to evaluate the magnitude of the conformational changes triggered upon inhibitor binding, the NS5B/inhibitor complex structures were compared with the existing native polymerase structure[8] (PDB code 1C2P). In the present analysis, one native and three NS5B/inhibitor complex structures accounting for eight crystallographically independent molecules were superimposed pair-wise. The r.m.s. deviations in 530 C^{α} positions between the native

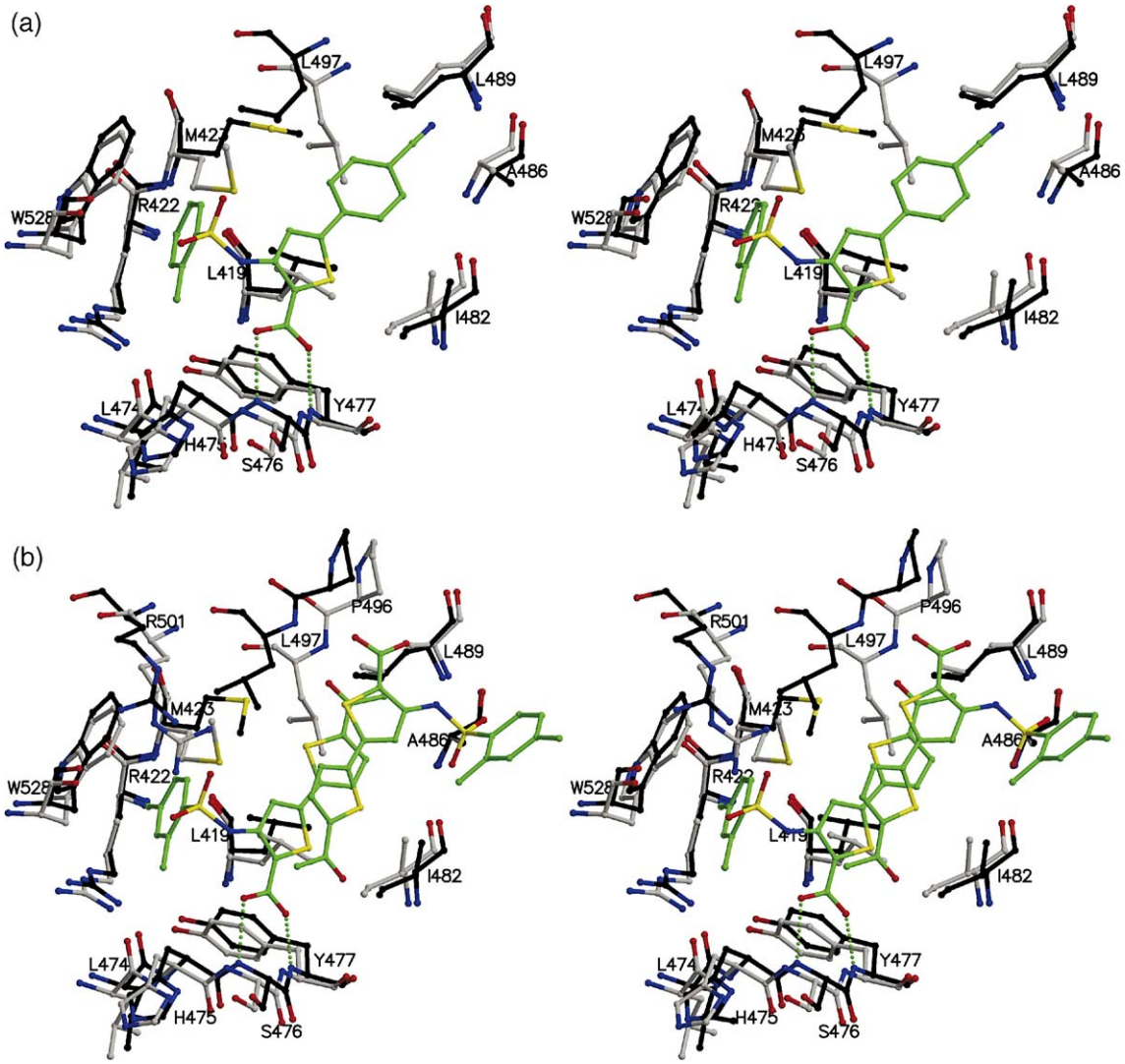

Figure 5. Stereo views of the conformational changes that occur at the NS5B inhibitor binding site upon (a) inhibitor B and (b) inhibitor C binding, with respect to the native NS5B molecule. Light grey and black correspond to the native and the inhibitor bound structures, respectively. The inhibitors are shown by ball and stick representation with carbon, nitrogen, oxygen and sulfur atoms in green, blue, red, and yellow, respectively. Two hydrogen bonds are shown in green.

and NS5B/inhibitor complex structures (Table 1) show clearly that the overall structure remains relatively unchanged upon inhibitor binding. However, unlike the phenylalanine-based inhibitors reported earlier,[30] the binding of the thiophene-based inhibitors induced conformational changes in some of the binding site residues (Figure 5(a) and (b); Table 2). This is due to the tighter binding of thiophene compounds as compared to the phenylalanine-based compounds. In particular, the number of van der Waals interactions between the NS5B and thiophene inhibitors is around 58–68, as compared to 43–49, between NS5B and phenylalanine inhibitors. All three inhibitors induce similar pocket residue perturbations. The common structural perturbations involve the side-chain of Met423 and the main-chain as well as the side-chain of the Leu497 (Figure 5(a) and (b)). The average displacement of the atoms of these residues is 3.5 Å. It is the change in the side-chain conformation of Met423 that triggers the perturbation; the movement of Leu497 produces a pronounced perturbation in the N-terminal residues of helix T of the thumb domain as can be seen in Figure 6(a). Residues Pro496–Arg505 constituting part of this helix, undergo a remarkable conformational change. The individual

Table 1. r.m.s. deviations (Å) in 530 C^{α} positions among the structures

	2	3	4
1	0.46–0.61 (0.52)	0.31–0.50 (0.42)	0.30–0.36 (0.33)
2		0.22–0.31 (0.25)	0.33–0.43 (0.38)
3			0.21–0.30 (0.25)

Since there are two crystallographically independent molecules in the crystal asymmetric unit that led to four possible ways of superimpositions, the minimum and maximum values of the deviations are given. The average value is given in parentheses. 1, Native NS5B polymerase; 2, NS5B/inhibitor A; 3, NS5B/inhibitor B; and 4, NS5B/inhibitor C structures.

Table 2. Deviations (Å) of C^{α} positions in the region Pro495-Arg505 of NS5B/inhibitor complex structures with respect to the native NS5B polymerase

Residues	NS5B/ inhibitor A	NS5B/ Inhibitor B	NS5B/ Inhibitor C
Pro495	0.60	0.57	0.65
Pro496	1.22	1.35	1.48
Leu497	1.81	2.01	2.31
Arg498	2.13	2.35	2.65
Val499	1.40	1.45	1.72
Trp500	0.80	0.86	1.07
Arg501	1.13	1.21	1.36
His502	1.42	1.48	1.85
Arg503	1.05	1.10	1.38
Ala504	0.48	0.59	0.75
Arg505	0.45	0.61	0.89

Each value is the average of four possible combinations of superimposition.

C^{α} atom deviations listed in Table 2 clearly demonstrate the magnitude of this rearrangement. Only the side-chain of Met423 and that of Leu497 interact directly with the inhibitor; since Leu497 is part of helix T, the displacement triggered by Met423 propagates in both directions of the polypeptide chain (Table 2 and Figure 6(a)). The movement can be described as roll of helix T about Val499 and Trp500. These perturbations most likely have an effect on the integrity of the allosteric GTP site[10] that is 17 Å from the non-nucleotide inhibitor binding site and is located on the opposite side of the highly positively charged helix T (Figure 6(b)).

Residues Ser29, Arg32, Pro495, Pro496, Val499 and Arg503 are involved in GTP recognition; these residues do not undergo any noticeable conformational change upon GTP binding.[10] The guanine base of GTP stacks against a hydrophobic platform provided by the side-chain of Pro495 and Val499, whilst the pyrrole ring of Pro496 is positioned perpendicular to the plane of the guanine base.[10] The $N^{\eta 2}$ atom of Arg503 interacts with the 2 amino group of the guanine base through water-mediated H-bonding interactions. The GTP binding at the interface of the thumb and finger domains possibly stabilizes the active conformation of the NS5B. Allosteric GTP binding has been reported by several laboratories to stimulate the initiation of RNA synthesis.[10,15,35–37] Other recent findings suggest that GTP-specific binding does not play a stimulatory role in *in vitro* RNA polymerase activity but is important for HCV RNA replication *in vivo*.[37] Similarly, no GTP effect was noticed in our assays as far as increased *in vitro* RNA replication or on NNI inhibition (results not shown). However, a very different picture emerges when residues interacting with GTP (Ser29, Arg32, Pro495, Pro496, Val499 and Arg503) are mutated and sub-genomic HCV RNA replication examined. Pro496Ala substitution reduces the efficiency of cell colony formation by approximately 60-fold.[37] Understandably, single mutations of Val499Gly, Arg503Lys, or Arg503Ala completely ablate the ability of sub-genomic HCV RNAs to replicate in cells, whereas other non-helix T interacting residue mutations such as Ser29 and Arg32 (part of helix A) only reduced the sub-genomic HCV RNA replication levels slightly.[37]

On the basis of the observed inhibitor-induced conformational changes, the genotype 2a structural studies[32] and the mounting literature support, we extend the explanation of the mechanism of action of our thiophene-based inhibitors in two directions. Firstly, the structural shifts of helix T most likely affect the integrity of the GTP binding site resulting in reduced affinity for GTP, thereby contributing to the formation of an RNA polymerase state incapable of carrying out a polymerization cycle. In addition, the shift in the position of helix T may destabilize the open/closed form of the polymerase dynamics needed for proper initiation, elongation and other complex *in vivo* RNA polymerase functions. Although it is only the side-chain of Met423 on helix Q that is perturbed, Met423 is in close proximity to helices S, T and A and these helices all have somewhat of an effect on the thumb/fingers interaction. It is conceivable, as seen for genotype 2a,[32] that the inhibitors lock the genotype 1b polymerase in the open inactive state and the β-hairpin-like conformation of the tip of the Λ1 loop cannot properly interact with the thumb domain to shift NS5B to the closed active form.

Secondly, there is evidence that the HCV polymerase may oligomerize in order to function.[38] His502 is one of the critical residues involved in homomeric interaction both at the *in vitro* and *in vivo* levels and mutating His502Glu abolishes the enzymatic activity. In the bound-state helix T environment, the position of His502 is greatly perturbed (Table 2) and the change certainly could have a profound effect on the interaction of the oligomerization process.

The C-terminal residues of NS5B play an important regulatory role in the enzymatic activity.[39–41] It has been reported that the C-terminally truncated forms of NS5B proteins enhance the polymerase enzymatic activity.[39–41] Since this region of NS5B does not undergo any noticeable conformational changes upon inhibitor binding, it is difficult to analyze the effect of NNIs on this region at the structural level. On the other hand, mutational studies involving the mutation of residues Trp500 to Arg505, that precede the C terminus, to alanine abolishes the enzymatic activity.[42] As discussed earlier, these residues forming a part of helix T, are shifted upon inhibitor binding, further reinforcing our inhibition mechanism.

Many NNIs of NS5B are allosteric and bind to the NS5B in specific non-overlapping binding sites.[27,30–33] Briefly, the structural basis of mechanisms of inhibition are (1) the stabilization of the β-loop.[27] (Leu443 to Ile454), (2) the disruption of inter-domain interactions[32,33] and (3) the perturbation of the GTP recognition site and disturbances in the oligomerization process (this paper). Hence, the potency of such inhibitors depends on the accessibility of such binding sites, which is also dependent on the dynamic conformational behavior of the polymerase

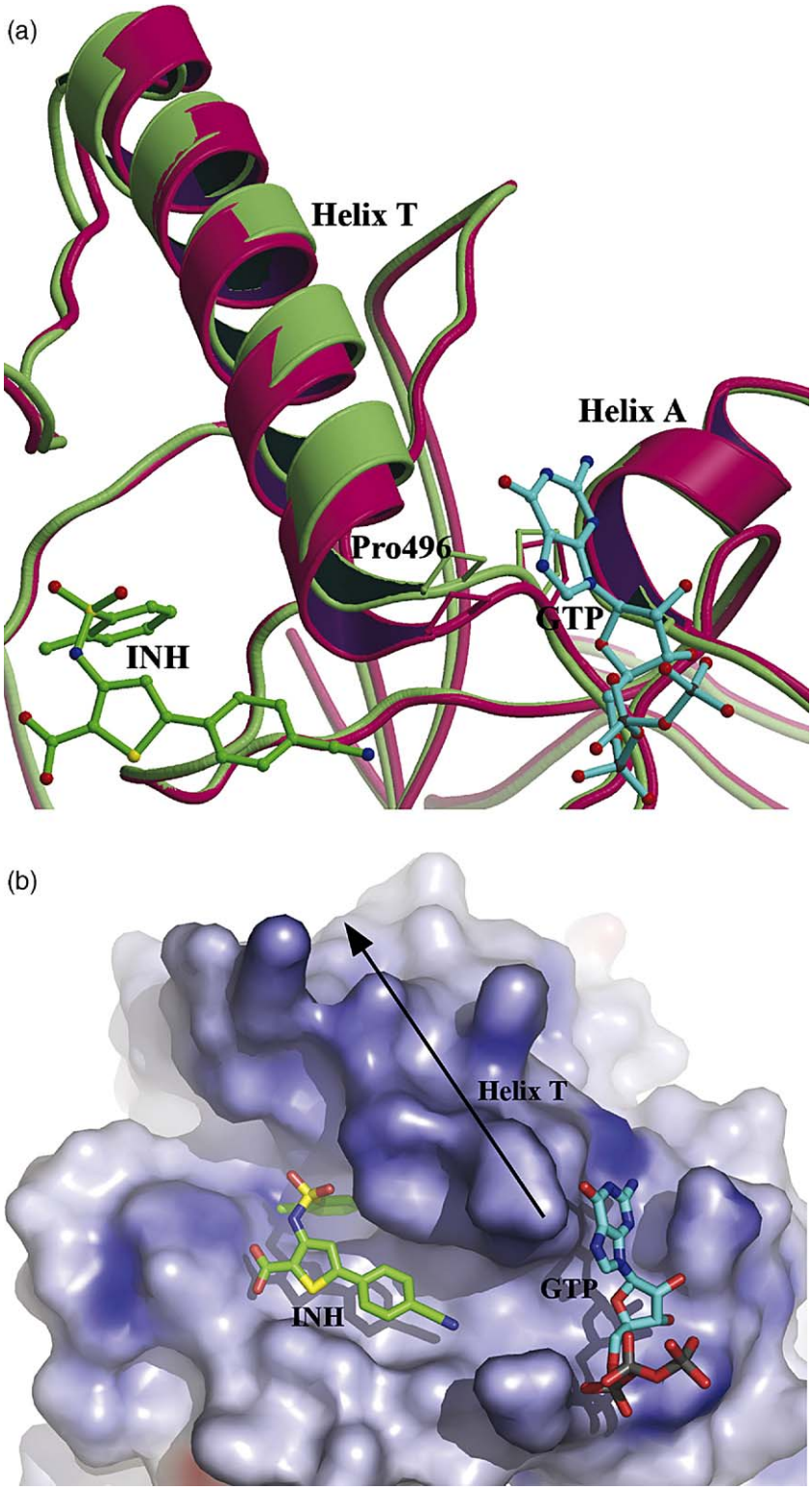

Figure 6. (a) Superimposition of NS5B/inhibitor B (light green) structure and the native NS5B structure (magenta), showing the conformational changes in the helix T. The inhibitor B (carbon, nitrogen, oxygen and sulfur atoms are shown in green, blue, red, and yellow, respectively) and GTP (carbon, nitrogen, oxygen and phosphorus atoms in green, blue, red, and gray, respectively) are shown in ball and stick representation. (b) The electrostatic potential surface showing the charge distribution of NS5B around the inhibitor and GTP binding sites. Blue color represents positive charge. The inhibitor and the GTP are shown by stick representation. Color codings are same as for (a).

during the polymerization cycles. Ma *et al.* have shown that NNIs including our previously reported thiophene compounds[23,24] are inactive against *in vitro* RNA replicase complex, of which NS5B forms a part, once the enzyme/template complex is preformed.[43] However, the potency of the NNIs presented here in the replicase complex is yet to be examined. It is conceivable that NNIs may inhibit the HCV NS5B prior to the formation of a stable enzyme/template complex through destabilization of polymerase/RNA interactions or disruption of important protein–protein contacts needed during replicase complex formation. In summary, our structural studies of NS5B polymerase with these thiophene-based inhibitors provide new insights into the current understanding of inhibition mechanisms of NS5B polymerase by non-nucleoside inhibitors.

Materials and Methods

Expression and purification of HCV NS5B protein

The recombinant form of the HCV genotype 1b NS5B is a 21 amino acid, C-terminal truncated version (Δ21) having an N-terminal hexahistidine tag. It was expressed in *Escherichia coli* BL21 (DE3) and purified as described by Ferrari *et al.*[44] and Lesburg *et al.*[8] with minor modifications. Briefly, the initial purification step consisted of loading soluble bacterial lysates onto a HiTrap nickel chelating affinity column (Amersham Biosciences, Baie d'Urfe, QC, Canada). Bound enzyme was eluted using an imidazole gradient. The polymerase fractions were pooled and the imidazole was removed using PD10 desalting columns (Amersham Biosciences). Further purification of the polymerase was performed by passing the nickel-NTA fractions through a HiTrap MonoS cation exchange column (Amersham Biosciences). Positive fractions were exchanged into a buffer containing 10 mM Tris (pH 7.5), 10% (v/v) glycerol, 5 mM DTT, 600 mM NaCl and glycerol was added to a final concentration of 40% for storage at −80 °C and subsequent activity and kinetic assays. For crystal structure study purposes, the enzyme was concentrated using an Ultra-15 Centrifugal Filter Unit (Millipore Ltd, Nepean, ON, Canada), precipitated with ammonium sulfate (Sigma-Aldrich Canada, Oakville, ON, Canada), and stored at 4 °C.

In vitro NS5B assay

Measurement of the inhibitory effects of compounds A, B and C on HCV NS5B genotype 1b polymerization activity was performed by evaluating the reduction in the amount of radiolabeled UTP incorporated by the enzyme into newly synthesized RNA using a homopolymeric RNA template/primer. Essentially, compounds were tested at various concentrations (0.024 to 50 μM) in a final volume of 50 μl reaction mixture consisting of 20 mM Tris–HCl (pH 7.5), 5 mM $MgCl_2$, 1 mM DTT, 50 mM NaCl, 500 ng of purified NS5B enzyme, 500 ng of poly(rA)/oligo(dT)$_{15}$ (Life Technologies, Burlington, ON, Canada), various concentrations of non-radioactive UTP (30 μM for the IC_{50} determination and 5 μM to 75 μM for the K_i determination), and 0.2 μCi to 3.1 μCi of (α-^{32}P)-labeled UTP (3000 Ci/mmol; Amersham Biosciences). RNA-dependent-RNA polymerase reactions were allowed to proceed for 50 min for IC_{50} determination or for 20 and 45 min for the K_i determination, at 22 °C. Reactions were stopped by the addition of 15 μl of 0.5 mM EDTA. Thereafter, volumes of 50 μl (25 μg) of sonicated salmon sperm DNA and 115 μl of a solution of 20% (w/v) trichloroacetic acid/0.5% (w/v)

Table 3. Data collection and refinement statistics

Crystal	Native	Complex A	Complex B	Complex C
Space group	$P2_12_12_1$	$P2_12_12_1$	$P2_12_12_1$	$P2_12_12_1$
a (Å)	86.02	84.75	84.93	85.53
b (Å)	105.90	106.13	104.31	105.98
c (Å)	127.13	127.44	127.01	126.61
Z	8	8	8	8
Matthews coefficient (Å^3/Da)	2.29	2.27	2.23	2.27
Solvent content (%)	46.3	45.7	44.7	45.8
A. *Data collection*				
Resolution (Å)	40.0–1.9	40.0–1.8	40.0–2.0	40.0–2.1
High resolution (Å)	1.97–1.9	1.86–1.8	2.07–2.0	2.18–2.1
Unique reflections	87,779	95,800	76,252	64,018
Multiplicity	3.5	3.0	4.3	4.0
$<I/\sigma(I)>$	23.3 (4.1)[a]	18.2 (3.5)	11.2 (3.3)	11.4 (3.7)
Completeness (%)	95.4 (73.6)	89.7 (92.1)	98.9 (96.3)	94.9 (75.6)
R_{sym} (%)[b]	4.8 (20.1)	4.7 (24.0)	8.0 (32.6)	7.4 (24.3)
B. *Refinement*				
Refinement resolution (Å)	40.0–1.9	40.0–1.8	40.0–2.0	40.0–2.1
Unique reflections (working/test)	83,343/4436	91,005/4795	72,236/3865	60,728/3233
$R_{working}/R_{free}$[c]	0.194/0.223	0.199/0.232	0.208/0.245	0.207/0.242
Number of residues	1119	1119	1119	1119
Number of water molecules	1007	1291	754	695
Average *B* factor (Å^2)[d]	21.1/–/34.7	20.4/25.1/34.4	28.8/29.5/34.3	27.5/26.7(57.6)/36.1
C. *r.m.s. deviations*				
Bond lengths (Å)	0.005	0.005	0.008	0.006
Bond angles (°)	1.2	1.2	1.4	1.2
Dihedral angles (°)	21.4	21.2	21.6	21.4
Improper angles (°)	0.75	0.74	0.84	0.75
D. *Ramachandran plot*				
Most favored regions (%)	91.6	91.5	92.0	89.9
Additional allowed regions (%)	8.3	8.4	7.9	10.1

[a] Values within the parentheses refer to the high resolution shell.
[b] $R_{sym} = \sum_h \sum_i (|I_i(h) - <I(h)>|) / \sum_h \sum_i I_i(h)$, where $I_i(h)$ is the i^{th} intensity measurement and $<I(h)>$ is the mean of all measurements of $I_i(h)$.
[c] $R_{working}$ and $R_{free} = \sum_h (|F(h)_{obs}| - |F(h)_{calc}|) / \sum_h |F(h)_{obs}|$ for reflections in the working and test sets. R_{free} was calculated using 5% of data.
[d] Average *B* factors of protein atoms, inhibitor atoms and water molecules, respectively. The value in the parenthesis is the average *B* factor of atoms of the second molecule of inhibitor C.

tetrasodium pyrophosphate at 4 °C were added to the mixture followed by incubation on ice for 30 min in order to ensure complete precipitation of nucleic acids. Samples were then transferred onto 96 well MultiScreen filter plates (Millipore Corp., Bedford, MA, USA). The filter plates were washed with 600 µl of 1% trichloroacetic acid/0.1% tetrasodium pyrophosphate per well and dried 20 min at 37 °C. A 50 µl volume of liquid scintillation cocktail (Wallac Oy, Turku, Finland) was added and the incorporated radioactivity was quantified using a liquid scintillation counter (Wallac MicroBeta Trilux, Perkin Elmer™, MA, USA). IC_{50} and K_i values were calculated using the computer software GraphPad Prizm (version 2.0; GraphPad Software Inc., San Diego, CA, USA).

Crystallization and data collection

Crystals were grown by the hanging drop method at room temperature, following the published protocol[8] with minor modifications. Three µl each of protein solution (HCV NS5B ΔC21 protein, 20 mg/ml in 5 mM 2-mercaptoethanol) and crystallizing agent solution (18% (w/v) PEG 4000, 0.3 M NaCl, 0.1 M sodium acetate buffer (pH 5.0), 5 mM 2-mercaptoethanol) were mixed on a cover slip and then equilibrated with a 1 ml reservoir of the precipitant solution. Diffraction quality crystals were obtained within one to three days by a macro seeding method.[45] Crystals belong to space group $P2_12_12_1$ with unit cell dimensions of $a = \sim 86$ Å, $b = \sim 105$ Å, and $c = \sim 126$ Å, values that are similar to published results.[8] The NS5B/inhibitor complexes were prepared by soaking the NS5B crystals in the inhibitor solutions for 10–12 h. The inhibitor solutions contained 3–5 mM inhibitor in 2–4% dimethyl sulfoxide (DMSO), 20% (w/v) PEG 4000, 50 mM NaCl, 10 mM $MgCl_2$, 5 mM mercaptoethanol, and 20 mM Tris buffer (pH 7.5).

Intensity data from the NS5B/inhibitor soaked crystals were collected at 105 K using an R-AXIS IV^{++} image plate detector with copper Kα radiation generated by a Rigaku RU-

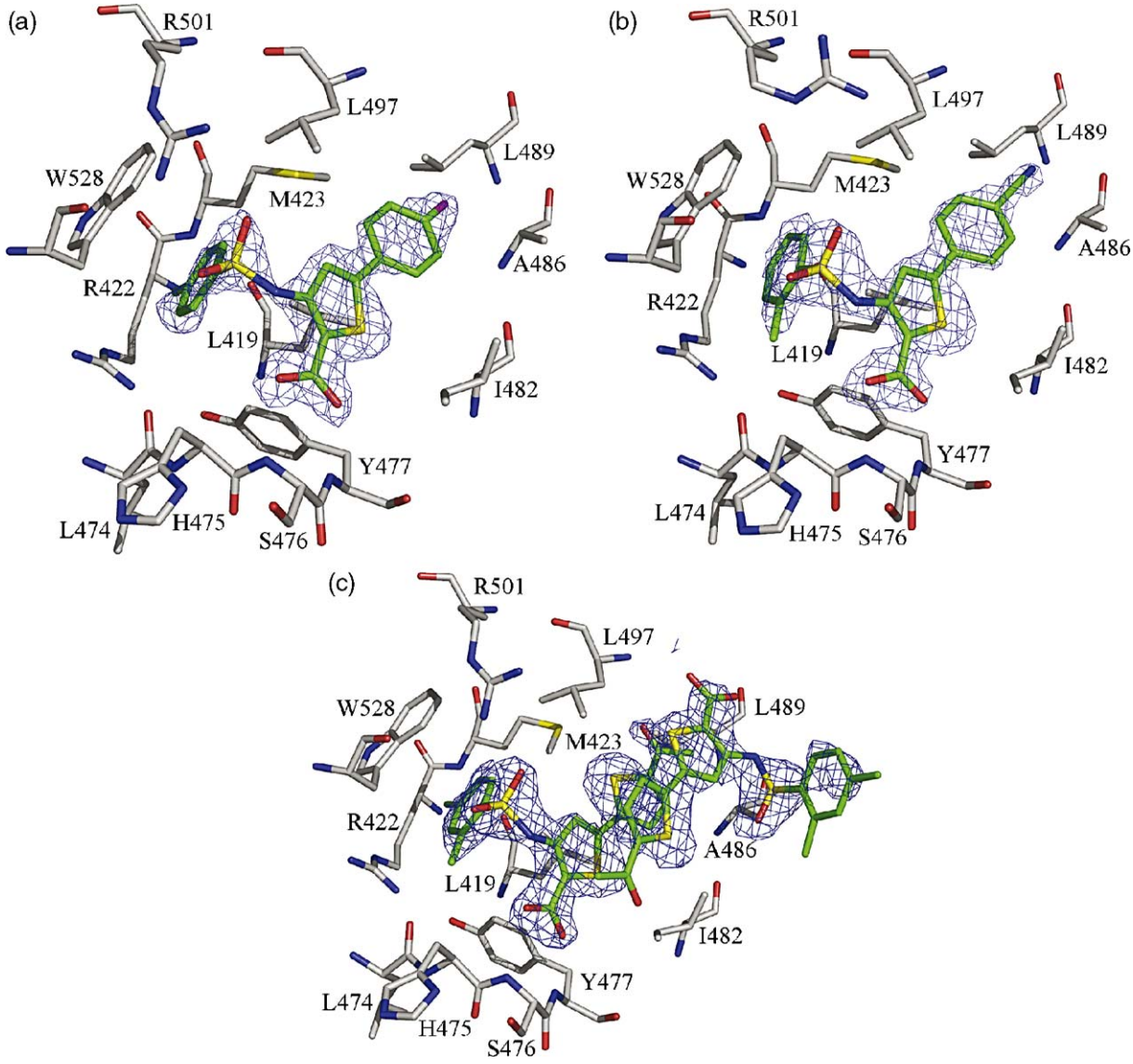

Figure 7. The initial difference electron density maps (blue) ($|F_{PI}|-|F_P|$, α_{calc}) contoured at the 3σ level at the inhibitor binding site, for (a) NS5B/inhibitor A, (b) NS5B/inhibitor B and (c) NS5B/inhibitor C complex structures, before the inhibitors were built. The final refined inhibitors were superimposed into their corresponding electron density maps. The inhibitors are shown by stick representation with color codings the same as that in Figure 3(a), (b) and (c).

300 rotating anode X-ray generator. The data sets were integrated and scaled using the programs DENZO and SCALEPACK.[46] Data collection statistics are given in Table 3.

Structure determination and refinement

The positioning of the two NS5B molecules in the asymmetric unit of the crystallographic unit cell was achieved by the molecular replacement method using the apopolymerase structure (PDB code 1C2P) as the search model. A difference Fourier map, $|F_{PI}|-|F_P|, \alpha_{calc}(|F_{PI}|$, structure factor amplitudes of the protein/inhibitor complex and $|F_P|$, structure factor amplitudes of the apo protein) permitted an initial positioning of the inhibitor molecule into the difference electron density (Figure 7(a), (b) and (c)). Structure refinement was carried out using the program CNS1.1.[47] All three NS5B/inhibitor complex structures reported herein were refined in the same manner. At the beginning, the model was subjected to 50 cycles of rigid body refinement treating each molecule as a rigid group. Subsequently, simulated annealing, positional, and individual *B*-factor refinements were performed. Model building, based on electron density maps ($2|F_o|-|F_c|$ at 1σ and $|F_o|-|F_c|$ at the 3σ contour levels), was performed wherever necessary using the program XtalView.[48] The R_{work} and R_{free} values were monitored closely throughout the refinement. Once the refinement had converged to a R_{work} value of 0.25, the identification of water molecules in the model was started. This was achieved in several cycles based on electron density peaks of at least 1σ in the $2|F_o|-|F_c|$ and 3σ in $|F_o|-|F_c|$ maps. Bulk solvent correction and anisotropic *B*-factor scaling were incorporated during the refinement. NCS restraints were not applied in the refinement. The stereochemical validity of the structures was examined using the program PROCHECK.[49] The detailed refinement statistics are given in Table 3.

Protein Data Bank accession codes

The final refined atomic coordinates of the NS5B/inhibitor complex structures have been deposited in the RCSB protein data bank (PDB accession codes are 2D3Z, 2D3U, and 2D41 for NS5B/inhibitors A, B, and C, respectively).

Structure analysis and generation of Figures

The buried surface area was calculated using the program CNS1.1.[47] Structural alignments were carried out by the program ALIGN.[50] Figures were generated by the programs MOLSCRIPT,[51] Raster3D,[52] and PYMOL†.

Acknowledgements

We thank the Alberta Heritage Foundation for Medical Research (AHFMR) for funding the purchase of the area detector facilities and the Canadian Institutes of Health Research (CIHR) for operating funds. M.N.G.J. is grateful for a Canada Research Chair in Protein Structure and Function. B.K.B. and M.M.C. acknowledge the generous support received from Virochem Pharma, Inc.

† http://www.pymol.org

References

1. Wasley, A. & Alter, M. J. (2000). Epidemiology of hepatitis C: geographic differences and temporal trends. *Semin. Liver Dis.* **20**, 1–16.
2. Pearlman, B. L. (2004). Hepatitis C treatment update. *Am. J. Med.* **117**, 344–352.
3. Kato, N., Hijikata, M., Ootsuyama, Y., Nakagawa, M., Ohkoshi, S., Sugimura, T. & Shimotohno, K. (1990). Molecular cloning of the human hepatitis C virus genome from Japanese patients with non-A, non-B hepatitis. *Proc. Natl Acad. Sci. USA*, **87**, 9524–9528.
4. Takamizawa, A., Mori, C., Fuke, I., Manabe, S., Murakami, S., Fujita, J. *et al.* (1991). Structure and organization of the hepatitis C virus genome isolated from human carriers. *J. Virol.* **65**, 1105–1113.
5. Grakoui, A., Wychowski, C., Lin, C., Feinstone, S. M. & Rice, C. M. (1993). Expression and identification of hepatitis C virus polyprotein cleavage products. *J. Virol.* **67**, 1385–1395.
6. Ago, H., Adachi, T., Yoshida, A., Yamamoto, M., Habuka, N., Yatsunami, K. & Miyano, M. (1999). Crystal structure of the RNA-dependent RNA polymerase of hepatitis C virus. *Structure Fold. Des.* **7**, 1417–1426.
7. Bressanelli, S., Tomei, L., Roussel, A., Incitti, I., Vitale, R. L., Mathieu, M. *et al.* (1999). Crystal structure of the RNA-dependent RNA polymerase of hepatitis C virus. *Proc. Natl Acad. Sci. USA*, **96**, 13034–13039.
8. Lesburg, C. A., Cable, M. B., Ferrari, E., Hong, Z., Mannarino, A. F. & Weber, P. C. (1999). Crystal structure of the RNA-dependent RNA polymerase from hepatitis C virus reveals a fully encircled active site. *Nature Struct. Biol.* **6**, 937–943.
9. O'Farrell, D., Trowbridge, R., Rowlands, D. & Jager, J. (2003). Substrate complexes of hepatitis C virus RNA polymerase (HC-J4): structural evidence for nucleotide import and de-novo initiation. *J. Mol. Biol.* **326**, 1025–1035.
10. Bressanelli, S., Tomei, L., Rey, F. A. & De Francesco, R. (2002). Structural analysis of the hepatitis C virus RNA polymerase in complex with ribonucleotides. *J. Virol.* **76**, 3482–3492.
11. Hansen, J. L., Long, A. M. & Schultz, S. C. (1997). Structure of the RNA-dependent RNA polymerase of poliovirus. *Structure*, **5**, 1109–1122.
12. Thompson, A. A. & Peersen, O. B. (2004). Structural basis for proteolysis-dependent activation of the poliovirus RNA-dependent RNA polymerase. *EMBO J.* **23**, 3462–3471.
13. Butcher, S. J., Grimes, J. M., Makeyev, E. V., Bamford, D. H. & Stuart, D. I. (2001). A mechanism for initiating RNA-dependent RNA polymerization. *Nature*, **410**, 235–240.
14. Ng, K. K., Cherney, M. M., Vazquez, A. L., Machin, A., Alonso, J. M., Parra, F. & James, M. N. (2002). Crystal structures of active and inactive conformations of a caliciviral RNA-dependent RNA polymerase. *J. Biol. Chem.* **277**, 1381–1387.
15. Choi, K. H., Groarke, J. M., Young, D. C., Kuhn, R. J., Smith, J. L., Pevear, D. C. & Rossmann, M. G. (2004). The structure of the RNA-dependent RNA polymerase from bovine viral diarrhea virus establishes the role of GTP in de novo initiation. *Proc. Natl Acad. Sci. USA*, **101**, 4425–4430.

16. Love, R. A., Maegley, K. A., Yu, X., Ferre, R. A., Lingardo, L. K., Diehl, W. *et al.* (2004). The crystal structure of the RNA-dependent RNA polymerase from human rhinovirus; a dual function target for common cold antiviral therapy. *Structure*, **12**, 1533–1544.
17. Appleby, T. C., Luecke, H., Shim, J. H., Wu, J. Z., Cheney, I. W., Zhong, W. *et al.* (2005). Crystal structure of complete rhinovirus RNA polymerase suggests front loading of protein primer. *J. Virol.* **79**, 277–288.
18. Dhanak, D., Duffy, K. J., Johnston, V. K., Lin-Goerke, J., Darcy, M., Shaw, A. N. *et al.* (2002). Identification and biological characterization of heterocyclic inhibitors of the hepatitis C virus RNA-dependent RNA polymerase. *J. Biol. Chem.* **277**, 38322–38327.
19. Tomei, L., Altamura, S., Bartholomew, L., Biroccio, A., Ceccacci, A., Pacini, L. *et al.* (2003). Mechanism of action and antiviral activity of benzimidazole-based allosteric inhibitors of the hepatitis C virus RNA-dependent RNA polymerase. *J. Virol.* **77**, 13225–13231.
20. Tomei, L., Altamura, S., Bartholomew, L., Bisbocci, M., Bailey, C., Bosserman, M. *et al.* (2004). Characterization of the inhibition of hepatitis C virus RNA replication by nonnucleosides. *J. Virol.* **78**, 938–946.
21. McKercher, G., Beaulieu, P. L., Lamarre, D., La Plante, S., Lefebvre, S., Pellerin, C. *et al.* (2004). Specific inhibitors of HCV polymerase identified using an NS5B with lower affinity for template/primer substrate. *Nucl. Acids Res.* **32**, 422–431.
22. Chan, L., Reddy, T. J., Proulx, M., Das, S. K., Pereira, O., Wang, W. *et al.* (2003). Identification of N,N-disubstituted phenylalanines as a novel class of inhibitors of hepatitis C NS5B polymerase. *J. Med. Chem.* **46**, 1283–1285.
23. Chan, L., Das, S. K., Reddy, T. J., Poisson, C., Proulx, M., Pereira, O. *et al.* (2004). Discovery of thiophene-2-carboxylic acids as potent inhibitors of HCV NS5B polymerase and HCV subgenomic RNA replication. Part 1: Sulfonamides. *Bioorg. Med. Chem. Letters*, **14**, 793–796.
24. Chan, L., Pereira, O., Reddy, T. J., Das, S. K., Poisson, C., Courchesne, M. *et al.* (2004). Discovery of thiophene-2-carboxylic acids as potent inhibitors of HCV NS5B polymerase and HCV subgenomic RNA replication. Part 2: tertiary amides. *Bioorg. Med. Chem. Letters*, **14**, 797–800.
25. Harper, S., Avolio, S., Pacini, B., Di Filippo, M., Altamura, S., Tomei, L. *et al.* (2005). Potent inhibitors of subgenomic hepatitis C virus RNA replication through optimization of indole-*N*-acetamide allosteric inhibitors of the viral NS5B polymerase. *J. Med. Chem.* **48**, 4547–4557.
26. Lee, G., Piper, D. E., Wang, Z., Anzola, J., Powers, J., Walker, N. & Li, Y. (2006). Novel inhibitors of hepatitis C virus RNA-dependent RNA polymerases. *J. Mol. Biol.* **357**, 1051–1057.
27. Powers, J. P., Piper, D. E., Li, Y., Mayorga, V., Anzola, J., Chen, J. M. *et al.* (2006). SAR and mode of action of novel non-nucleoside inhibitors of hepatitis C NS5B RNA polymerase. *J. Med. Chem.* **49**, 1034–1046.
28. Tedesco, R., Shaw, A. N., Bambal, R., Chai, D., Concha, N. O., Darcy, M. G. *et al.* (2006). 3-(1,1-dioxo-2H-(1,2,4)-benzothiadiazin-3-yl)-4-hydroxy-2(1H)-quinolinones, potent inhibitors of hepatitis C virus RNA-dependent RNA polymerase. *J. Med. Chem.* **49**, 971–983.
29. Koch, U., Attenni, B., Malancona, S., Colarusso, S., Conte, I., Di Filippo, M. *et al.* (2006). 2-(2-Thienyl)-5,6-dihydroxy-4-carboxypyrimidines as inhibitors of the hepatitis C virus NS5B polymerase: discovery, SAR, modeling, and mutagenesis. *J. Med. Chem.* **49**, 1693–1705.
30. Wang, M., Ng, K. K., Cherney, M. M., Chan, L., Yannopoulos, C. G., Bedard, J. *et al.* (2003). Nonnucleoside analogue inhibitors bind to an allosteric site on HCV NS5B polymerase: crystal structures and mechanism of inhibition. *J. Biol. Chem.* **278**, 9489–9495.
31. Love, R. A., Parge, H. E., Yu, X., Hickey, M. J., Diehl, W., Gao, J. *et al.* (2003). Crystallographic identification of a non-competitive inhibitor binding site on the hepatitis C virus NS5B RNA polymerase enzyme. *J. Virol.* **77**, 7575–7581.
32. Biswal, B. K., Cherney, M. M., Wang, M., Chan, L., Yannopoulos, C. G., Bilimoria, D. *et al.* (2005). Crystal structures of the RNA-dependent RNA polymerase genotype 2a of hepatitis C virus reveal two conformations and suggest mechanisms of inhibition by non-nucleoside inhibitors. *J. Biol. Chem.* **280**, 18202–18210.
33. Di Marco, S., Volpari, C., Tomei, L., Altamura, S., Harper, S., Narjes, F. *et al.* (2005). Interdomain communication in hepatitis C virus polymerase abolished by small molecule inhibitors bound to a novel allosteric site. *J. Biol. Chem.* **280**, 29765–29770.
34. De Francesco, R. & Migliaccio, G. (2005). Challenges and successes in developing new therapies for hepatitis C. *Nature*, **436**, 953–960.
35. Lohmann, V., Overton, H. & Bartenschlager, R. (1999). Selective stimulation of hepatitis C virus and pestivirus NS5B RNA polymerase activity by GTP. *J. Biol. Chem.* **274**, 10807–10815.
36. Luo, G., Hamatake, R. K., Mathis, D. M., Racela, J., Rigat, K. L., Lemm, J. & Colonno, R. J. (2000). *De novo* initiation of RNA synthesis by the RNA-dependent RNA polymerase (NS5B) of hepatitis C virus. *J. Virol.* **74**, 851–863.
37. Cai, Z., Yi, M., Zhang, C. & Luo, G. (2005). Mutagenesis analysis of the rGTP-specific binding site of hepatitis C virus RNA-dependent RNA polymerase. *J. Virol.* **79**, 11607–11617.
38. Qin, W., Luo, H., Nomura, T., Hayashi, N., Yamashita, T. & Murakami, S. (2002). Oligomeric interaction of hepatitis C virus NS5B is critical for catalytic activity of RNA-dependent RNA polymerase. *J. Biol. Chem.* **277**, 2132–2137.
39. Tomei, L., Vitale, R. L., Incitti, I., Serafini, S., Altamura, S., Vitelli, A. & De Francesco, R. (2000). Biochemical characterization of a hepatitis C virus RNA-dependent RNA polymerase mutant lacking the C-terminal hydrophobic sequence. *J. Gen. Virol.* **81**, 759–767.
40. Adachi, T., Ago, H., Habuka, N., Okuda, K., Komatsu, M., Ikeda, S. & Yatsunami, K. (2002). The essential role of C-terminal residues in regulating the activity of hepatitis C virus RNA-dependent RNA polymerase. *Biochim. Biophys. Acta*, **1601**, 38–48.
41. Leveque, V. J., Johnson, R. B., Parsons, S., Ren, J., Xie, C., Zhang, F. & Wang, Q. M. (2003). Identification of a C-terminal regulatory motif in hepatitis C virus RNA-dependent RNA polymerase: structural and biochemical analysis. *J. Virol.* **77**, 9020–9028.
42. Yamashita, T., Kaneko, S., Shirota, Y., Qin, W., Nomura, T., Kobayashi, K. & Murakami, S. (1998). RNA-dependent RNA polymerase activity of the soluble recombinant hepatitis C virus NS5B protein truncated at the C-terminal region. *J. Biol. Chem.* **273**, 15479–15486.
43. Ma, H., Leveque, V., De Witte, A., Li, W., Hendricks, T., Clausen, S. M. *et al.* (2005). Inhibition of native hepatitis C virus replicase by nucleotide and non-nucleoside inhibitors. *Virology*, **332**, 8–15.

44. Ferrari, E., Wright-Minogue, J., Fang, J. W., Baroudy, B. M., Lau, J. Y. & Hong, Z. (1999). Characterization of soluble hepatitis C virus RNA-dependent RNA polymerase expressed in *Escherichia coli*. *J. Virol.* **73**, 1649–1654.
45. Stura, E. A. & Wilson, I. A. (1991). Seeding Techniques. In *Crystallization of Nucleic Acids and Proteins: A Practical Approach* (Ducruix, A. & Giege, G., eds), IRL Press, Oxford.
46. Otwinowski, Z. & Minor, W. (1997). Processing X-ray diffraction data collected in oscillation mode. *Methods Enzymol.* **276**, 307–326.
47. Brunger, A. T., Adams, P. D., Clore, G. M., DeLano, W. L., Gros, P., Grosse-Kunstleve, R. W. *et al.* (1998). Crystallography and NMR system: A new software suite for macromolecular structure determination. *Acta Crystallog. sect. D*, **54**, 905–921.
48. McRee, D. E. (1999). XtalView/Xfit—A versatile program for manipulating atomic coordinates and electron density. *J. Struct. Biol.* **125**, 156–165.
49. Laskowski, R. J., MacArthur, M. W., Moss, D. S. & Thornton, J. M. (1993). PROCHECK: a program to check the stereochemical quality of protein structure. *J. Appl. Crystallog.* **26**, 283–291.
50. Cohen, G. H. (1997). ALIGN: a program to superimpose protein coordinates, accounting for insertions and deletions. *J Appl. Crystallog.* **30**, 1160–1161.
51. Kraulis, P. J. (1991). MOLSCRIPT: a program to produce both detailed and schematic plots of protein structures. *J. Appl. Crystallog.* **24**, 946–950.
52. Merritt, E. A. & Murphy, M. E. (1994). Raster3D Version 2.0. A program for photorealistic molecular graphics. *Acta Crystallog. sect. D*, **50**, 869–873.

Edited by I. Wilson

(Received 28 March 2006; received in revised form 30 May 2006; accepted 31 May 2006)
Available online 16 June 2006